Advective transport of CO_2 in permeable media induced by atmospheric pressure fluctuations: 2. Observational evidence under snowpacks

W. J. Massman[1] and J. M. Frank[1]

Received 13 January 2006; revised 12 April 2006; accepted 18 May 2006; published 28 July 2006.

[1] Meadow and forest CO_2 amounts sampled beneath an approximately meter deep (steady state) snowpack at a subalpine site in southern Rocky Mountains of Wyoming are observed to vary by nearly 200 ppm over periods ranging from 4 to 15 days. This work employs the model of periodic, pressure-induced, advective transport in permeable media developed in part 1 of this study to investigate these CO_2 fluctuations. With the aid of this physically based model, inferences are made about the nature of the physical properties of both the forcing mechanism and the snowpack that contribute to these periodic variations in undersnow CO_2. Results are consistent with the hypothesis that the undersnow CO_2 is being driven by advective flows induced by pressure fields created when the wind interacts with the local aerodynamic roughness elements (nearby mountain peaks, forest edges, snowdrifts). Nonharmonic spectral and cospectral techniques indicate that the wind modulates the low-frequency temporal dynamics of the undersnow CO_2, whereas comparisons of the modeled and observed time lag between the surface forcing and the response of the undersnow CO_2 suggest that site topography determines the horizontal structure of the wind (surface pressure) forcing. It is also suggested here that the snowpack is at most a weakly dispersive medium. Finally, because the model includes a CO_2 source term in the soil underlying the snowpack, other findings suggest that both the wintertime CO_2 fluxes emanating from the snowpack and the soil respiration rates may vary significantly between a meadow soil and a forest soil at this site.

Citation: Massman, W. J., and J. M. Frank (2006), Advective transport of CO_2 in permeable media induced by atmospheric pressure fluctuations: 2. Observational evidence under snowpacks, *J. Geophys. Res.*, *111*, G03005, doi:10.1029/2006JG000164.

1. Introduction

[2] Part 1 of this study [*Massman*, 2006] develops an analytical model of soil or snowpack CO_2 response to periodic pressure forcing at the surface of the substrate. The model was developed for both dispersive and nondispersive media by decomposing the mass flow (the advective-diffusive and dispersive-diffusive) equations into a steady state component and a sinusoidally, time-varying component using the Fourier or spectral decomposition technique. Physical constraints on the amplitude of the time-dependent component indicate that the mathematical decomposition technique follows a perturbation type approach. Part 1 also derived and discussed the diffusive flux enhancement factors appropriate to dispersive and nondispersive media.

[3] This part (part 2) of the study uses the analytical model to compare modeled and observed time lags between sinusoidal forcing at the surface of a deep snowpack and the response of the CO_2 measured at the interface between the snowpack and the soil. In general terms, any observed time lag, or phase lag as it is sometimes called, is determined by the frequency and strength of the forcing and the physical properties of the medium. For example, when surface pressure decreases, the flux of CO_2 or other trace gases from the soil will tend to increase in response [*Schery et al.*, 1984; *Holford et al.*, 1993; *Chen et al.*, 1995]. Thus near the surface the CO_2 amounts will initially decrease, but ultimately the amounts of CO_2 at all levels throughout the substrate will vary in time depending on the amount of CO_2 stored in the substrate (as indicated by the model CO_2 vertical profile) and the distribution of the CO_2 sources within the substrate [*Massman*, 2006]. Furthermore, as the frequency of the forcing decreases the deeper the wave will penetrate into the substrate [*Auer et al.*, 1996; *Massman*, 2006]. Consequently, the phase lag at any given depth is simply the time required for the surface perturbation to propagate to that depth.

[4] Both *Lewicki et al.* [2003] and *Takagi et al.* [2005] performed a time lag analysis in their studies of CO_2 efflux from natural environments. *Lewicki et al.* [2003], studying the shallow soils along the San Andreas and Calaveras Faults of California, found that changes in the CO_2 efflux lagged about half an hour behind the forcing by wind speed, whereas *Takagi et al.* [2005], studying a snow covered

[1]Rocky Mountain Research Station, USDA Forest Service, Fort Collins, Colorado, USA.

forest in northern Japan, found that the maximum CO_2 fluxes (measured by eddy covariance) lagged behind wind events between about 1.5 and 4 hours. Additionally, *Lewicki et al.* [2003] also found that the forcing was better described by variations in wind speed rather than pressure fluctuations. Because *Lewicki et al.* [2003] were studying the rate of CO_2 emanating from the surface, the half-hour time lag they observed suggests that at least the near-surface CO_2 responds quite quickly. The study of *Takagi et al.* [2005] was focused more on CO_2 at some depth into the substrate, which can be expected to respond more slowly than for shallow substrates. Like *Takagi et al.* [2005], this study is focused on CO_2 under a snowpack of about 1 m depth.

[5] However, unlike *Lewicki et al.* [2003] or *Takagi et al.* [2005], the present study models the time lag associated with specific forcing frequencies. In this study the observed time lags are modeled by adjusting two model parameters (the horizontal wavelength of the forcing, k_h, and the dispersivity of the medium, α) so that the modeled time lags are made to approximate the observed time lags. In turn, this allows inferences to be made as to the nature of the forcing and the dispersivity of the medium.

[6] The remainder of this paper is divided into three sections. The next section details the site description and the methods used for data analysis. Following that, section 3 examines whether the wind speed or the barometric pressure is better suited for modeling the forcing variable and compares the measured and modeled time lags. Section 3 also provides estimates of the wintertime soil CO_2 source strength and the effects that pressure pumping can have on the CO_2 fluxes emanating from the snowpack. The final section summarizes the conclusions of this study.

2. Methods

2.1. Site Description and Field Measurements

[7] Data for this study were obtained between 19 December 2000 and 8 February 2001 at the Glacier Lakes Ecosystem Experiments Site (GLEES) (41°20′N, 106°20′W), an alpine/subalpine ecosystem (elevation 3186 m) located in the Rocky Mountains of southern Wyoming about 70 km west of Laramie, Wyoming. The study period corresponds to the first 50.5 days of the undersnow CO_2 experiment described by *Musselman et al.* [2005], who provide more details concerning the GLEES site and the pressure, wind, and undersnow CO_2 data. Here we summarize the key points relevant to the use of the analytical pressure forcing model described in part 1 [*Massman*, 2006].

[8] For these particular days the mean ambient pressure was 68.5 kPa, the average wind speed at 32 m above the surface was 7.5 m s^{-1}, and the snowpack depth (D_w) at the two CO_2 sampling positions [*Musselman et al.*, 2005] was about 1.1 m at the meadow location and 0.7 m at the forest location. These two sampling locations were separated by about 20 m. Wind speed and direction were obtained by an RM Young propeller-vane anemometer (RM 0S103-5) and the ambient pressure was obtained with a Vaisala pressure transducer (AIR AB-2AX) located about 30 m above the surface. The wind and pressure data were obtained every 5 min and averaged to produce half-hourly values. Snow depth was determined weekly by direct measurement with a preinstalled depth marker (pole) anchored into the soil. The CO_2 samples were replicated at both the meadow and forest sites using CO_2 collectors (screened cylindrical volumes attached to tubes) that had been placed on the soil surface during the summer of 2000. During the winter the snow was allowed to accumulate undisturbed over the collectors. Each of the four CO_2 measurements was obtained from a 30-s sample taken every half hour by drawing the sample through a decabond tube into a Li-COR 6262. The flow rate was about 8 L min^{-1}, and the 6262 sample rate was 5 Hz. The sample lag time was about 6 s for the meadow site and 12 s for the forest site. Of the 150 or so CO_2 measurements obtained during each of these 30 s sampling periods, this study focuses on those few that occur within 0.5 s or so after the lag time [*Musselman et al.*, 2005]. At the meadow site the mean or steady state undersnow CO_2 for the 50.5 days of the experiment was 1532 ppm. At the forest site it was 779 ppm. Ambient atmospheric CO_2 mol fraction was about 375 ppm.

[9] During this period the snow depth was remarkably and atypically constant, as shown in more detail in section 3. This is critical for this study because as snow depth increases the undersnow CO_2 also increases [*Musselman et al.*, 2005]. Consequently, significant changes in snow depth could obscure or interfere with the CO_2 variations associated with pressure forcing. Still, there remains the need to estimate a fixed set of model parameter values to describe the snowpack and soil, both of which can be spatially structured and, in the case of snow, temporally dynamic.

[10] Because no detailed measurements of the snow or soil physical properties are available during this initial portion of the experiment, we will rely on data obtained from a nearby location during an earlier experiment on natural pressure forcing in snow [*Massman et al.*, 1997]. Consequently, for snow we will assume that the porosity of the snow $\eta_w = 2/3$ and that the tortuosity of the snow $\tau_w = 0.85$. These values are about the average values obtained for the previous experiment. In the earlier study, *Massman et al.* [1997] used the model of *Sommerfeld and Rocchio* [1993] to estimate the snow permeability (k_w) from the bulk density measurements. However, we found when comparing to other observations of snow permeability [e.g., *Shimizu*, 1970; *Albert et al.*, 2000] that this model may underestimate k_w somewhat. Furthermore, in the previous experiment the snow pack was definitely layered because the grain size varied by an order of magnitude over the depth of the snowpack, suggesting that the snow permeability can easily vary by 1 or 2 orders of magnitude within the present snowpack. However, combining the models and the observations suggested that $k_w = 6.25 \times 10^{-9}$ m^2 is a reasonable, but highly uncertain, estimate of the snow permeability for the present study.

[11] In addition to any spatial variablity, the snowpack and its associated physical parameters do naturally vary with time as the snowpack undergoes settling and metamorphism. Undoubtedly then, over the course of the 50.5 days of this study period the snow properties are likely to have changed. Small amounts of snow did fall throughout this period, and there were many sunny days which would have warmed and sublimated the snow surface. Ice lenses do form in this area, but they are uncommon during midwinter, as studied here. There is no evidence for their

presence or absence during the experiment, so we assume that they were not present during the study period. Nevertheless, 2 weeks before the beginning date of the study period the snow depth was 1.25 m in the meadow and about 0.8 m in the forest. Therefore during the 14-day period preceding the nearly steady state snow depth period the snowpack had undergone some change. However, after this 2-week period the bulk density of snow may not have changed much because it is not a particularly dynamic quantity after about a week or so of falling [e.g., *Lundy et al.*, 2002]. In turn, this may have stabilized the porosity and permeability somewhat [e.g., *Shimizu*, 1970; *Sommerfeld and Rocchio*, 1993]. These values for the physical properties are assumed constant throughout the study period, so that we can simplify the snowpack to a one-layer steady state snowpack.

[12] In general, the soils at this site are thin, rocky, relatively undeveloped, and, at this time of year, fairly dry. Since the forest and meadow sites discussed in this study are near the location of the previous soil samples [*Massman et al.*, 1997], we assign the soil depth $D_l = 0.7$ m, the soil porosity $\eta_l = 2/3$, and the soil permeability $k_l = 1.40 \times 10^{-11}$ m^2. This particular value of k_l is the average of the values obtained from the previous experiment. The soil tortuosity, τ_l, is unknown. However, models of tortuosity, such as those of *Neale and Nader* [1973] and *Millington* [1959], suggest that for a dry soil that $\tau_l \approx \tau_w$, while the model of *Du Plessis and Masliyah* [1991], suggests that $\tau_l \approx 0.9\ \tau_w$. However, these and other models of soil tortuosity depend upon assumptions about the shape of the particles and their geometric arrangement within the medium, so that other models could give rather different estimates for τ_l. For convenience we will assume that $\tau_l = \tau_w$. Given the imprecision associated with these choices for the model snowpack and soil parameters, a sensitivity analysis is included as part of this study to evaluate the uncertainty in any predicted lag time.

2.2. Data Analyses

[13] Central to the use of the analytical model developed in part 1 [*Massman*, 2006] are the frequencies and amplitudes of the forcing (snow surface pressure) and the response (undersnow CO_2) and the phase or time lag between them. These model parameters were determined from the measured wind, pressure, and CO_2 time series using a nonharmonic spectral analysis (NHSA) technique [*Padmanabhan*, 1991; *Schickedanz and Bowen*, 1977]. The advantage the NHSA has over the traditional Fourier Transform or Fast Fourier Transform is better resolution of the frequency content of a time series. With the nonharmonic method the search for periodic behavior includes both harmonics of the fundamental and frequencies between the harmonics. The NHSA used in this study is implemented as follows.

[14] The basis functions, S_{mn} and C_{mn}, are computed first.

$$S_{mn} = \sin(2\pi mn/N) \tag{1}$$

$$C_{mn} = \cos(2\pi mn/N), \tag{2}$$

where N is the total number of (equally spaced) data points in the time series; $n = 1, 2, \cdots, N$; and m can take on any real value between 1 and the integer part of $N/2$. That is $m \in \mathcal{R} \ni 1 \le m \le [N/2]$. In this study we divide every interval between successive integers, j and $j + 1$, into 9 equal subintervals so that within this (open) interval m takes on the values of $j + 0.1, j + 0.2, \cdots, j + 0.9$. The number of subintervals is arbitrary, but nine is sufficient for the present purposes and it also keeps the computational overhead low. The frequency of the mth waveform is $\omega_m = 2\pi\ m/(N\Delta t)$, where Δt is the sampling interval, and the associated period is $(N\Delta t)/m$.

[15] Second, the basis functions are used in a regression with a set of observations, X_n, to estimate the coefficients a_m, b_m, and c_m of each mth waveform.

$$X_n = a_m + b_m S_{mn} + c_m C_{mn} + \epsilon(n), \tag{3}$$

where $\epsilon(n)$ is the residual. Next, the coefficient of determination, R_m^2, is computed for each waveform.

$$R_m^2 = 1 - \sum_{n=1}^{N} \left(X_n - \hat{X}_{mn}\right)^2 / \sum_{n=1}^{N} \left(X_n - \overline{X}\right)^2, \tag{4}$$

where $\overline{X}$ is the mean of X_n and $\hat{X}_{mn} = a_m + b_m S_{mn} + c_m C_{mn}$. The distribution of R_m^2 with frequency forms the spectrum. It is important to note that whenever m takes on a noninteger value the basis functions are not orthogonal so they are correlated. Practically speaking this may render the spectral estimates less reliable. However, this problem can be diagnosed by calculating the correlation coefficients and checking for significance using standard tests employed in multiple linear regression and correlation analyses [*Schickedanz and Bowen*, 1977]. For the present study, which focuses on identifying the first few frequencies of each time series, this issue was found to be of little concern.

[16] The final step in the analysis is to remove the waveform associated with the highest R_m^2 value from the time series. That is, we compute a new time series, $X_n^{(1)} = X_n - \hat{X}_{in}$, where $\hat{X}_{in}$ is the single waveform associated with the maximal value in R_m^2. The NHSA is then repeated on the new time series, $X_n^{(1)}$, using the same (precalculated) basis functions. The new spectrum is then searched for its maximal R_m^2 value, the coefficients tested for significance, and again a new time series is constructed by removing the dominant waveform form from $X_n^{(1)}$ to produce $X_n^{(2)}$. This procedure is iterated until several (or l in total) dominant frequencies have been identified. The final spectrum then is simply the set of l elements of the m values associated with each of the dominant frequencies. A final R^2 value is also computed using the set of dominant waveforms, which gives the fraction of the total variance of the original time series explained by the set of l waveforms.

[17] The NHSA is effective at constructing a spectrum for any given time series. However, the spectral content will not necessarily be the same for different time series. Highly divergent spectra for wind or pressure and the undersnow CO_2 mol fraction would suggest either that the CO_2 response to the forcing is highly nonlinear, which is what would be expected if the response frequencies differ significantly from the forcing frequencies, or that there is no real

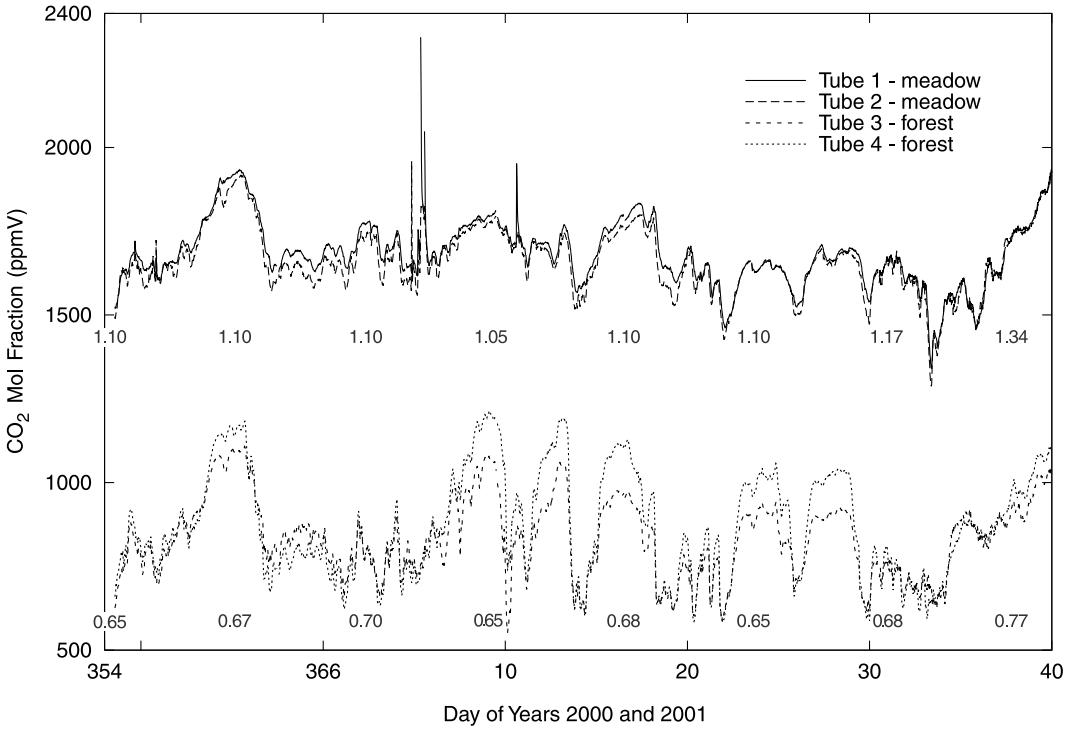

Figure 1. Time course of the undersnow CO_2 measurements at the meadow and forest sites for the 50.5 days of the experiment. Replicates at both sites are included. Weekly snow depth observations (m) at each site are given by the series of numbers beneath the CO_2 graphs.

connection between the (presumed) forcing and undersnow CO_2 response. In the event that the forcing and response time series have similar spectral content (even if the relative importance of the dominant frequencies is different), then it is possible to surmise that the undersnow CO_2 is in fact responding to the forcing. Certainly this is what would be expected from the analytical model outlined in part 1 of this study [*Massman*, 2006]. Therefore, in order to apply the analytical model, the forcing and response frequencies should be exactly the same. This can be accomplished by constructing a nonharmonic cospectrum (NHC), which can be obtained by combining the information from the two nonharmonic spectra.

[18] The NHC is constructed in much the same way as the nonharmonic spectra, as follows. For any individual time series the amplitude of each wave form is $A_m = \sqrt{b_m^2 + c_m^2}$ and the associated phase is $\phi_m = N \arctan(b_m/c_m)/(2\pi m)$. The NHC is then (proportional to) $A_m(1)A_m(2)\cos(\Delta\phi_m)$, where $A_m(1)$ is the amplitude of the mth waveform of the first time series, $A_m(2)$ is for the second time series, and $\Delta\phi_m$ is the difference between the phases of the two waveforms. Once the same frequencies for both forcing and response have been clearly identified, then the time lag between the two waveforms, $\Delta t\Delta\phi_m$, is the desired (or measured) time lag between the forcing and the CO_2 response. For comparative purposes the normalized square cospectral (NSC_m) values are also provided. The NSC_m is just the $NHC^2/[VAR(1)VAR(2)]$; where VAR(J) is the variance of the first or second time series determined by squaring and summing the amplitudes from the corresponding nonharmonic spectra, i.e., $VAR(J) = \Sigma_m A_m^2(J)$ and J = 1 or 2. The NSC_m is useful for determining the relative ranking of the forcing-response waveforms.

3. Results and Discussion

3.1. Characterizing the Forcing

[19] The physically based models discussed in part 1 of this study [*Massman*, 2006] clearly indicate that surface pressure is a key driving variable for causing advective flows in permeable media. However, this variable is not often measured in studies of pressure effects in soils or snowpacks, so a surrogate is needed. This section examines whether wind or ambient pressure is the better surrogate.

[20] Figure 1 shows the replicated undersnow CO_2 measurements from 19 December 2000 (Day 354) through 9 February 2001 (Day 40) for both the meadow and forest sites. Generally speaking, the undersnow CO_2 amounts are greater at the meadow site because the snow is deeper there. The data used in this study begin in the afternoon of day 354 of year 2000 and end at midnight of day 38 of year 2001, or N = 2422 half-hourly observations. These data clearly indicate that the undersnow CO_2 is quite dynamic and can vary 10% to 20% within a few days. The question being addressed in the present study is whether these fluctuations are caused by or are consistent with pressure-induced advective flows within the snowpack and soil.

[21] Figure 1 also includes the weekly snow depths measured at each site. On day 30 (2001) the snow depth had increased slightly to 1.17 m from a nearly steady value of about 1.10 m. This increase was probably associated with drifting, rather than any significant snow fall. Such a small increase in snow depth is unlikely to have had much impact

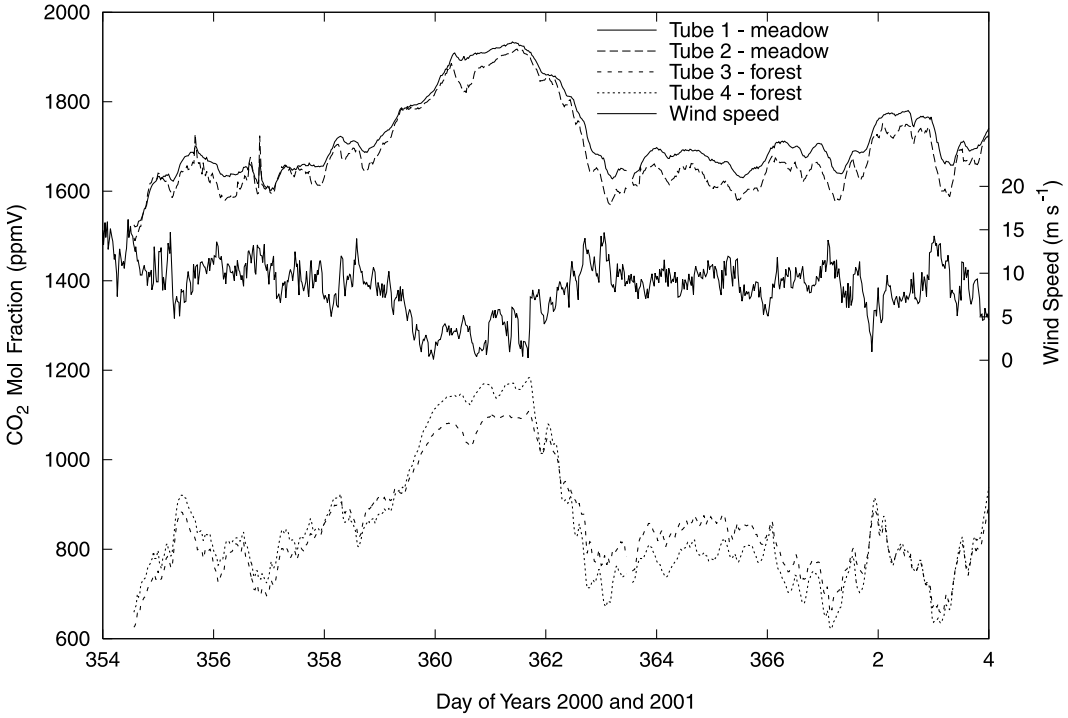

Figure 2. Time course of wind speed and undersnow CO_2 measurements for the first 2 weeks of the experiment.

on the undersnow CO_2 because the undersnow CO_2 decreased a few days later to the lowest level recorded during the observation period. This suggests that other forcing was still influencing the undersnow CO_2 because, in general, undersnow CO_2 increases (not decreases) as the snow depth increases [*Musselman et al.*, 2005]. The last snow depth was taken the afternoon of day 37, shortly after snow had begun to fall. The snow continued for sometime after day 38 and the concomitant increase in snow depth is likely to have influenced the undersnow CO_2 amounts. However, during this snowfall period the pressure dropped about 0.8 kPa, while the wind speed dropped from about 12 m s^{-1} to less than 4 m s^{-1}, it then increased to 10 m s^{-1} before dropping to near 0 m s^{-1}. Consequently, the undersnow CO_2 was also being forced by these other factors as well. Furthermore the undersnow CO_2 response is not instantaneous to any of these forcing factors, so it is not possible to tell precisely what role the increasing snow depth and the advective effects played during the last 48 hours of so of the 1211 hours of observation. For this study we assume that the advective effects are contributing significantly enough during the snowy period to include them in the ensuing analysis. This assumption was (at least partially) verified by performing the same type of analysis on the data set that did not include the last 48 hours (N = 2326). For the purposes of identifying the nature of the forcing function and the forcing frequencies, the results were nearly identical with the N = 2422 case.

[22] Figures 2 and 3 show the first 2 weeks of the undersnow data along with either the wind speed (Figure 2) or the ambient pressure (Figure 3). The most important and most prominent feature of these two figures is the significant variation in the undersnow CO_2 between days 359 and 363. The amplitude of this perturbation in the CO_2 is over 200 ppm at both the meadow and forest sites. Comparing Figures 2 and 3 suggests that during this 4-day event, increasing (decreasing) undersnow CO_2 lags behind decreasing (increasing) wind speed, but that no such obvious pattern appears with the ambient pressure. A careful examination of Figure 2 also suggests that a similar forcing/response pattern between wind speed and the undersnow CO_2 also occurs at periods shorter than the major 4-day event. These comparisons suggest that for the present study, wind speed is a better measure of advective forcing than is the ambient pressure.

[23] The correlation coefficients (r_{12}) between the undersnow CO_2 and the wind speed and ambient pressure support the possibility that wind speed is the forcing function even more convincingly than a simple visual inspection. For tubes 1 through 4, r_{12} (in order) = −0.472, −0.550, −0.618, and −0.726 for wind speed, whereas for ambient pressure, r_{12} = +0.078, +0.122, +0.057, and −0.036. The correlation between the undersnow CO_2 and wind speed is much stronger than it is for CO_2 and ambient pressure. *Lewicki et al.* [2003] demonstrated a similar result in their study of soil CO_2.

[24] Forcing by wind speed is also supported by the nonharmonic spectral analysis, which are listed in Table 1. (Note that the spectra for tubes 2 and 4 are not included in this table because they are so similar to tubes 1 and 3 that they are not needed.) These results indicate that the structures of the spectra associated with the undersnow CO_2 resemble the wind speed spectrum more closely than they resemble the ambient pressure spectrum. For example, only waveform index 1 occurs in the pressure spectrum and both undersnow CO_2 spectra. Likewise, waveform index 12.5 of

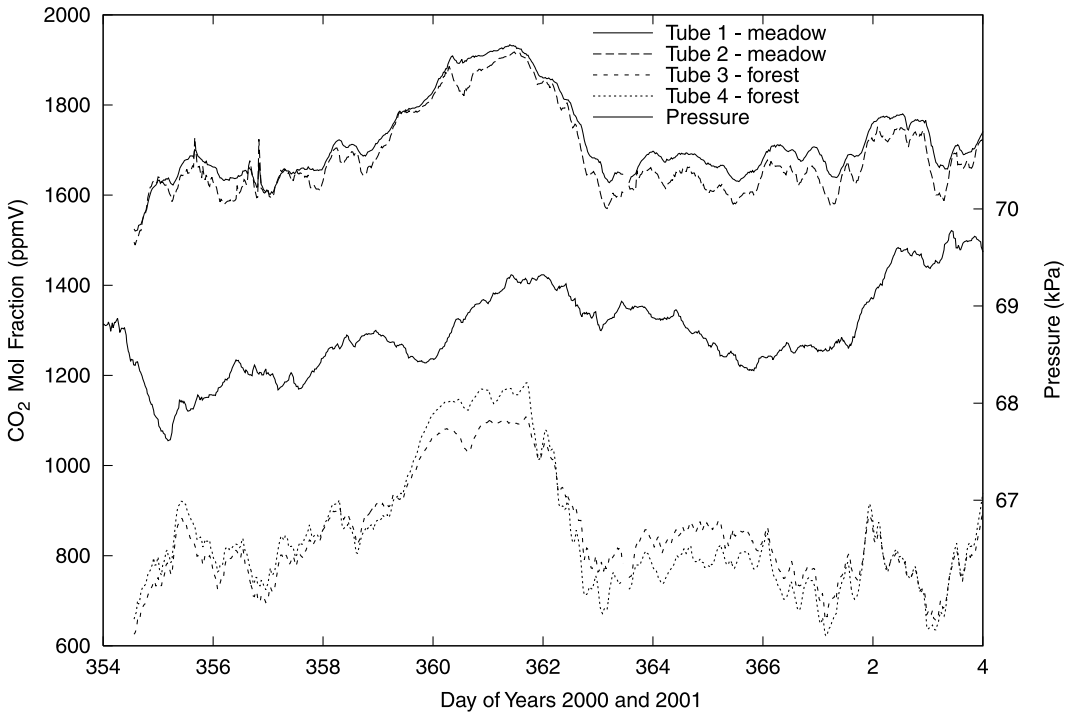

Figure 3. Time course of pressure and undersnow CO_2 measurements for the first 2 weeks of the experiment.

the ambient pressure and waveform index 12.1 of the forest undersnow CO_2 are similar enough that they may represent the same waveform. However, the wind speed and the undersnow CO_2 spectra share the following (approximate) waveform indices 1.1 ± 0.1, 3.2 ± 0.2, 4.6 ± 0.2, 7.1 ± 0.2, 9 ± 0.1, and 13.6 ± 0.2. Therefore, assuming that the undersnow CO_2 is responding linearly to the forcing, i.e., that response frequencies are the same as the forcing frequencies, then wind speed better describes the frequency content of the forcing than does the ambient pressure. In accordance with this and the evidence previously presented, we will assume that the wind speed is the driving force behind the variations in the observed undersnow CO_2.

[25] This result should not be too surprising. The GLEES area, which encompasses mountains, patchy forests with openings varying between a few meters to more than 100 m, snow drifts, and boulders throughout the region, is quite aerodynamically rough. The undersnow CO_2 is probably responding to a variety of local pressure fields created as the wind interacts with these various roughness objects. *Lewicki et al.* [2003] hypothesized the same physical mechanism when explaining their soil CO_2 fluxes. This issue will be discussed again when comparing the modeled and observed lag times between the forcing and the CO_2 response.

[26] In order to compare the CO_2 observations with *Massman*'s [2006] linear model of advective forcing the forcing and response frequencies should be equal. In the case of the NHSA (Table 1) the frequencies associated with the wind speed are not quite the same as those associated with either of the undersnow CO_2 sites. For identifying specific and identical forcing and response frequencies, the NHC is required. Table 2 lists the five dominant nonharmonic cospectral waveform indices associated with the results provided by Table 1. The dominant NHC frequencies are very similar to those that occurred in Table 1. Furthermore, in the case of the wind speed the five dominant frequencies of the NHC are nearly identical for both the meadow and forest sites. However, the relative ranking of the first three frequencies is different for each site. Table 2 also includes the results for the waveform corresponding to a period of about 2 days (waveform index ≈26 has a period of 47 hours). This particular waveform, although it is relatively weak compared to the other more dominant waveforms, is included here because it will also be used in the comparison between the measured and modeled phase lag.

[27] All frequencies listed in Tables 1 and 2 and indicate that the relatively low frequency atmospheric phenomena are

Table 1. Nonharmonic Spectral Analyses of the Meadow (Tube 1) and Forest (Tube 3) Undersnow CO_2, the Horizontal Wind Speed, and the Ambient Pressure[a]

Meadow CO_2 m [R_{cum}^2]	Forest CO_2 m [R_{cum}^2]	Wind Speed m [R_{cum}^2]	Ambient Pressure m [R_{cum}^2]
1 [*0.26*]	3.4 [*0.27*]	6.9 [*0.16*]	5.2 [*0.20*]
4.5 [*0.49*]	4.7 [*0.36*]	3.2 [*0.27*]	2.5 [*0.39*]
6.9 [*0.60*]	13.4 [*0.45*]	1.2 [*0.37*]	1 [*0.54*]
13.8 [*0.66*]	12.1 [*0.51*]	13.7 [*0.45*]	3.9 [*0.68*]
1.9 [*0.70*]	7.3 [*0.57*]	12.3 [*0.49*]	8 [*0.76*]
3.2 [*0.73*]	1 [*0.61*]	4.8 [*0.53*]	16 [*0.80*]
9.1 [*0.75*]	8.9 [*0.64*]	26.1 [*0.56*]	12.5 [*0.83*]
26 [*0.77*]	2.4 [*0.67*]	9 [*0.59*]	10.6 [*0.86*]

[a]The first eight dominant waveforms of each are listed and are denoted by the waveform index, m. The waveforms are ranked in order of importance. The cumulative R^2 (the fraction of the total variance explained by the sum of the waveforms) is given in italics and enclosed in the square brackets [R_{cum}^2]. The period associated with each waveform is $1211/m$ (hours).

Table 2. Waveform Indices (m) Determined From Nonharmonic Cospectral Analysis Between the Meadow (Tube 1) and Forest (Tube 3) Undersnow CO_2 and the Horizontal Wind Speed and the Meadow and Forest Undersnow CO_2 and the Ambient Pressure[a]

Meadow CO_2 Wind Speed m [NSC_m]	Forest CO_2 Wind Speed m [NSC_m]	Meadow CO_2 Ambient Pressure m [NSC_m]	Forest CO_2 Ambient Pressure m [NSC_m]
4.5 [*0.072*]	3.3 [*0.093*]	1 [*0.137*]	1.1 [*0.028*]
6.9 [*0.061*]	7 [*0.037*]	3 [*0.020*]	2.9 [*0.026*]
3.2 [*0.046*]	4.7 [*0.034*]	4.7 [*0.010*]	3.8 [*0.006*]
13.8 [*0.011*]	13.8 [*0.018*]	1.7 [*0.008*]	5.1 [*0.006*]
1.2 [*0.008*]	1.2 [*0.006*]	6.4 [*0.005*]	12.6 [*0.005*]
26 [*0.002*]	26 [*0.002*]	26.1 [*0.0001*]	26.3 [*0.0007*]

[a]A normalized value of the cospectral power corresponding to the waveform index (frequency) is given in italics and enclosed in the square brackets [NSC_m]. (Note that the values of NSC_m included in this table can be compared to one another, but they cannot be compared to either an R^2 or the cumulative R^2, R^2_{cum}, in Table 1.) The first five waveforms are included above the blank row and they are ranked in the order of importance. The approximate 2-day period waveform (m = 26) is included below the blank row to indicate that other more significant waveforms have been deleted from the list. The period associated with each waveform is 1211/m (hours).

responsible for the forcing. For example, the period associated with waveform index, m, is about 50.5/m days, indicating that higher waveform indices have shorter periods. The results shown in Table 2 indicate that atmospheric motions with periods greater than 3.7 (50.5/13.8) days are responsible for most of the undersnow CO_2 forcing. Because this frequency range is typically associated with low-frequency synoptic-scale atmospheric motions, most of the variability in the undersnow CO_2 is likely to be the result of barometric pumping. Furthermore, this is true for forcing by either the wind speed or the ambient pressure. Although the correlation between ambient pressure and undersnow CO_2 response is weak, the ambient pressure NHC also display some of the same forcing frequencies as the wind speed. In particular the frequencies 1.1, 3 and 4.7 are quite similar to 1.2, 3.2, and 4.7 that occur in the wind speed NHC. Furthermore, the strongest forcing of the undersnow CO_2 ($NSC_{m=1}$ = 0.137) appears to be associated with pressure at the meadow site. (Note, too, that all other pressure forcing appears to be very weak by comparison to this one particular pressure waveform or to most of the wind speed waveforms.) It is possible, therefore, that the atmospheric forcing is a mixture of pressure variations and wind speed fluctuations. However, by necessity the remainder of this study focuses solely on wind speed forcing.

[28] Before turning to the time lags, there are some important inferences about linear and nonlinear forcing and response that can be taken from Tables 1 and 2. First, the slight differences in frequencies between the forcing and the CO_2 response (Table 1) may indicate that the CO_2 response is weakly nonlinear. However, further exploration of this type of nonlinear response is beyond the intent of this study. Second, Table 2 indicates that waveforms 6.9 and 13.8 contribute to both the CO_2/wind speed cospectra. However, because 13.8 = 2(6.9), it is an "overtone" (an integer multiple) of 6.9. The presence of an overtone in the NHC can indicate a nonlinearity in either the forcing or the response or both. Table 1 indicates that the wind speed displays this overtone, because both 6.9 and 13.7 are present. Consequently, at a minimum the forcing appears to be somewhat nonlinear. On the other hand, Table 1 also indicates that the same overtone appears with the meadow CO_2. However, we cannot be certain whether the undersnow CO_2 is responding linearly to nonlinear forcing or whether it is responding nonlinearly to linear forcing. Nevertheless, it is more reasonable to assume the former (i.e., linear response to nonlinear forcing) because the model developed in part 1 suggests that for any given forcing frequency we should expect the same response frequency. That is, to first order the response is always linear. On the other hand, a nonlinear response would be indicated if, for example, the spectrum associated with the forcing did not include the "overtone" index 13.8 and the response spectrum did. In this case the nonlinearity would be the sole property of the response. For this study we assume that the response is linear because to do so is consistent with the modeling results and to do otherwise cannot be readily justified.

3.2. Measured and Modeled Time Lags

[29] For comparisons between the modeled and measured time lags, we focus on the frequencies corresponding to the waveforms 4.5, 6.9 and 26 (Table 2). Table 3 lists the observed and model estimated time lags between the wind forcing and undersnow CO_2 response for the meadow site. Table 4 lists the results for the forest site. The forcing frequency, ω, corresponding to waveform 4.5 is 6.6×10^{-6} Hz, for 6.9 it is 1.0×10^{-5} Hz, and for 26 it is 3.7×10^{-5} Hz. The uncertainty associated with these

Table 3. Measured and Modeled Time Lags Between the Assumed Forcing (Wind Speed) and the Undersnow CO_2 Response at the Meadow Site[a]

Waveform ω, Hz	Waveform Period, Hours	$A_{\chi 1}(D_w)$, ppm	Observed Lag Time, Hours	ND Lag Time, Hours	HD Lag Time, Hours	WD Lag Time, Hours	Horizontal Wavelength, km
6.6×10^{-6}	264	59	140 ± 2	85 ± 4	73 ± 4	82	100
				108	91	105	10
				151 ± 4	138 ± 4	148	1
1.0×10^{-5}	174	42	99 ± 2	61 ± 3	50 ± 4	58	100
				72	58	69	10
				104 ± 3	93 ± 3	102	1
3.7×10^{-5}	47	17	28 ± 1	20 ± 1	17 ± 1	20	100
				21	17	20	10
				32 ± 1	28 ± 1	32	1

[a]Here ND means nondispersive, HD means highly dispersive, and WD means weakly dispersive. Snow depth at this site is 1.1 m.

Table 4. Measured and Modeled Time Lags Between the Assumed Forcing (Wind Speed) and the Undersnow CO_2 Response at the Forest Site[a]

Waveform ω, Hz	Waveform Period, Hours	$A_{\chi_1}(D_w)$, ppm	Observed Lag Time, Hours	ND Lag Time, Hours	HD Lag Time, Hours	WD Lag Time, Hours	Horizontal Wavelength, km
6.6×10^{-6}	264	45	115 ± 2	76 ± 3	70 ± 2	75	100
				92	81	90	10
				142 ± 2	134 ± 2	140	1
1.0×10^{-5}	174	35	83 ± 3	54 ± 3	48 ± 2	52	100
				61	52	59	10
				97 ± 2	89 ± 1	95	1
3.7×10^{-5}	47	23	26 ± 1	18 ± 1	15 ± 1	18	100
				19	15	18	10
				29 ± 1	25 ± 1	29	1

[a]Here ND means nondispersive, HD means highly dispersive, and WD means weakly dispersive. Snow depth at this site is 0.7 m.

specific values is at most ±5% for the two lowest frequencies and at most about ±10% highest frequency.

[30] Tables 3 and 4 also include the estimates of the uncertainties in the model time lags associated with imprecision in the model values of snow and soil porosity, tortuosity, and permeability. Snow and soil porosity and tortuosity were varied by ±10%. The snow permeability was varied by a factor of 2. (Note that the soil permeability is not included here because it had very little influence on the time lag.) However, the variations in these parameters were done synergistically to produce the maximum variation in model time lag. Furthermore, the model sensitivity to these parameters is shown only for the bounding conditions (i.e., nondispersive and highly dispersive media for long and short wavelength forcing). For this range of model parameters the maximum range of variation in the model lag time is about 4 hours, which is no more than about a 5% uncertainty in relative measure and is comparable in absolute measure to the uncertainty associated with the observed lag time. The NHSA of the undersnow CO_2 provided the estimate of the amplitude of the (sinusoidal) undersnow CO_2 response, $A_{\chi_1}(D_w)$. The boundary conditions at the snow surface were fixed at $A_p(0) = 10$ Pa for the amplitude of the sinusoidal forcing and $A_{\chi_1}(0) = 1$ ppm was assumed for the sinusoidal amplitude of CO_2 field. (See Part I for a fuller explanation of the notation and interpretation of these three model-related amplitudes). The influence of this particular choice of values for the upper boundary conditions was tested by varying them both by 2 orders of magnitude. Their influence on the modeled time lag was insignificant.

[31] Included in Tables 3 and 4 are the model lag times for three different assumptions of snow dispersivity (nondispersive, highly dispersive, and weakly dispersive) and three different horizontal wavelengths associated with the forcing. However, the dispersion coefficient, $\mathcal{D}$ ($m^2\ s^{-1}$), is proportional to both the dispersivity of the medium, α, and the horizontal wave number of the forcing, k_h ($=2\pi/\lambda_h$, where λ_h is the horizontal wavelength) [*Massman*, 2006]. Consequently, for a dispersive medium (with a fixed value for the dispersion coefficient, $\mathcal{D}$) α and k_h cannot be varied independently. For the present study "a highly dispersive medium" means $\mathcal{D} \approx 2\ D_e$, where D_e ($m^2\ s^{-1}$) is the diffusivity of CO_2 in air corrected for the tortuosity and porosity of the medium. "A weakly dispersive medium" means $\mathcal{D} \approx 0.2\ D_e$. As a result, a highly dispersive medium satisfies the condition $\alpha k_h = 2\pi \times 10^{-3}$ and a weakly dispersive medium satisfies $\alpha k_h = 2\pi \times 10^{-4}$.

[32] There are five observations concerning the results listed in Tables 3 and 4 that should be mentioned. First, the lag time between the surface forcing and response can be several hours (or days) for such low-frequency motions. Second, the lag time decreases as $\mathcal{D}$ increases, which is to be expected because dispersion acts to enhance diffusion. Third, results from both sites suggest that time lag decreases as the depth of the medium decreases. Again, this is not unexpected because, as presented earlier, the variations in the undersnow CO_2 are more strongly correlated with wind speed at the forest site than they are at the meadow site. Thereore one would expect the forest site to be more strongly coupled to the forcing. Fourth, the horizontal wavelength of the forcing that best "fits" the observed lag times appears to be between about 2 and 5 km. (Note we suggest the 2–5 km range rather than 1–10 km because 2–5 km provides a tighter bound on the observed time lags than 1–10 km.) This is considerably shorter than the 10^3–10^4 km wavelength one might expect with such low forcing frequencies. However, if, as hypothesized earlier, the forcing is related local to pressure fields caused by the wind interacting with the site roughness elements, then $\lambda_h \approx 2$–5 km may reflect the scale of important roughness features in the terrain and the forest in the GLEES area. Another way of expressing this is that the variations in wind speed, which during the wintertime at GLEES occur as a result of low-frequency atmospheric motions, act primarily to modulate (intensify and diminish) the locally generated drag- and turbulence-related pressure fields. Thus the pressure-induced advective forcing within the snowpack might then be related more closely to a modulated standing wave phenomenon rather than a traveling wave. One candidate for a modulated standing wave with a 2–5 km wavelength is a mountain lee wave forced by the topography. While these inferences concerning a standing wave type of forcing are reasonable, they must be understood only as consistent with the data so they remain speculative. Assuming that the 2–5 km range is approximately correct, then fifth, the observed time lags at both sites are obviously consistent with either a nondispersive or a weakly dispersive medium; that is, the predictions bound the observations. Likewise by the same test, the forest snowpack may also be consistent with the possibility of being highly dispersive, except possibly at higher frequencies. However, for the meadow

snowpack to be highly dispersive, either the horizontal wavelength would have to be about 1 km or less or the snowpack would have to be have a higher dispersivity than assumed in the model. Maybe the proximity of the meadow site to the edge of the forest (a discontinuity in the local roughness) exposes the meadow site to more turbulence and shorter wavelength motions. Another possibility is that the forest site is somewhat more dispersive than the meadow site. This issue regarding whether these snowpacks are highly dispersive cannot be resolved with the current data set. Therefore the best and maybe the most consistent scenario for interpreting the observations is that these GLEES snowpacks are at best weakly dispersive and that the wavelength associated with the forcing is about 2–5 km.

3.3. Model of the GLEES Snowpack CO_2 Efflux

[33] So far this study has focused on using the analytical model developed in part 1 to simulate the lag time between the atmospheric forcing (pressure pumping) and the under-snow CO_2 response for individual fixed frequencies. Ultimately, however, the analytical model's utility lies in its ability to simulate CO_2 fluxes across the spectrum of pressure forcing. Section 7.3 of part 1 of the present study outlined how this integration across the turbulent pressure spectrum was carried out for R_{wave}, the enhancement factor caused by the interaction of the forcing and response waves. This section (1) extends the results for R_{wave} to low-frequency barometric pumping and (2) provides simplified expressions for the model (wave-enhanced and dispersive) fluxes. The next section summarizes the numerical estimates of the CO_2 advectively enhanced fluxes appropriate to the low-frequency forcing discussed in the preceding sections of this paper.

[34] The total vertical CO_2 flux emanating from the upper surface of the snowpack, $\overline{F}_\chi(0)$, is the sum of the diffusional flux, $F_{diff}(0)$, the wave flux, $F_{wave}(0)$, and the gradient-dispersive flux, $F_{gd}(0)$, which results from the pressure forcing interacting with the mean flow through the coefficient of dispersivity as discussed in part 1. (Note that the notation for these fluxes and the enhancement factors, which are introduced next, are the same as in part 1.) For the present purposes, $\overline{F}_\chi(0)$ is written as

$$\overline{F}_\chi(0) = F_{diff}(0) + \left[R^{turb}_{wave} + R^{baro}_{wave}\right]F_{diff}(0) + \left[R^{turb}_{disp} + R^{baro}_{disp}\right]F_{diff}(0), \quad (5)$$

where R refers generically to an enhancement factor, the subscript refers to either the wave or the dispersive components of the enhancement, and the superscript signifies either high-frequency turbulent forcing or low-frequency barometric forcing. R_{wave} is defined in part 1. R_{disp} is simply the ratio of the coefficient of dispersion to the effective diffusivity, i.e., $R_{disp} = \mathcal{D}/D_e$, and as such is mathematically distinct from R_{wave}. The separation of R into high- and low-frequency components is largely for convenience of the simplifications and is intended to indicate that the limits of the spectral integration are different for high and low frequencies. The spectral shape of the pressure forcing and the limits of integration over high-frequency turbulent forcing are detailed in part 1. For the low-frequency forcing we use the same modeled pressure spectra, but we integrate over wave motions with periods 6 hours or longer. For the high-frequency forcing we used Taylor's hypothesis to relate the horizontal wavelength of the waveform to its frequency. For the low frequencies we assumed that the horizontal wavelength of the waveform was independent of its driving frequency, in accordance with the findings discussed in the previous section and suggested by the wavelengths listed in Tables 3 and 4.

[35] The integration was performed numerically for each of the four enhancement factors, yielding

$$R^{turb}_{wave} = f_{cs}\left[\frac{\sigma^2_{p,turb}(0)k_w^2}{\mu^2\nu^2}\right]\left[\frac{k_w K_{wave}}{u^2}\right], \quad (6)$$

$$R^{baro}_{wave} \approx 0, \quad (7)$$

$$R^{turb}_{disp} = \left[\frac{3}{4}\alpha k_h\right]\left[\frac{\sigma_{p,turb}(0)k_w}{\mu D_e}\right]\left[\frac{K_{disp}}{u}\right], \quad (8)$$

$$R^{baro}_{disp} = \left[\frac{3}{4}\alpha k_h\right]\left[\frac{\sigma_{p,baro}(0)k_w}{\mu D_e}\right], \quad (9)$$

where f_{cs} is the nondimensional scaling factor associated with the substrate pore geometry (see equations (31) and (32) of part 1), $\sigma^2_{p,turb}(0)$ (Pa^2) is the variance of the turbulent pressure fluctuations at the upper surface of the snowpack, μ (Pa s) is the dynamic viscosity of air, ν ($m^2\ s^{-1}$) is the kinematic viscosity of air, u (m s^{-1}) is the horizontal wind speed, $\sigma_{p,baro}(0)$ (Pa) is the root-mean-square of the low-frequency barometric pressure variance at the surface of the snowpack, K_{wave} ($\approx$4.0 s^{-2}) is a constant, and K_{disp} ($\approx$1.8 m s^{-1}) is a constant. Since we have no observational data with which to estimate the turbulent fluxes, we use R^{baro}_{disp} in the next section to estimate the dispersive fluxes. However, recall that for this study a highly dispersive medium satisfies the condition $\alpha k_h = 2\pi \times 10^{-3}$, while a weakly dispersive medium satisfies $\alpha k_h = 2\pi \times 10^{-4}$, and that $\sigma_{p,\ baro}(0)$ is assigned a fixed value of 10 Pa.

[36] Before closing this section we should point out that previous studies have used or developed relationships between the horizontal wind speed and the amplitude of the pressure forcing ($\sigma_p(0)$ or $A_p(0)$). Such relationships are important because they can be used to estimate $\sigma_{p,baro}(0)$ or $A_p(0)$, which for some types of low-frequency atmospheric motions may or may not be easily measured.

[37] *Waddington et al.* [1996] suggested wind blowing over "wavy" topography, would yield the following pressure amplitude:

$$A_p(0) = \frac{1}{2}\rho_{air}u^2_{10}(Hk_h), \quad (10)$$

where ρ_{air} is the density of the ambient air, u_{10} is the horizontal wind speed measured at 10 m above the "wavy" topography, and H is the height of the "wavy" topography above the otherwise flat surface. For this example, H is likely to be limited to a few meters at most. Assuming that

Table 5. Strength of the Meadow and Forest Soil CO_2 Source Term (or Soil Respiration Rates) and the Fluxes Inferred From the Steady State CO_2 Model Developed by *Massman* [2006][a]

Site	ND Source Strength, μmol-CO_2 m^{-3} s^{-1}	HD Source Strength, μmol-CO_2 m^{-3} s^{-1}	WD Source Strength, μmol-CO_2 m^{-3} s^{-1}
Meadow	0.51	1.31	0.59
Forest	0.28	0.72	0.33
	Diffusional Flux, μmol-CO_2 m^{-2} s^{-1}	Total Flux, μmol-CO_2 m^{-2} s^{-1}	Total Flux, μmol-CO_2 m^{-2} s^{-1}
Meadow	0.37	0.93	0.41
Forest	0.20	0.52	0.23

[a]The total flux is diffusional flux plus the gradient dispersive flux. See *Massman* [2006] for details on the gradient dispersive flux. Here ND means

the topography causes a propagating wave (in which case H can be a few hundred meters), then mountain wave theory [*Nappo*, 2002] suggests that

$$A_p(0) = \rho_{air} u_0 H \sqrt{N^2 - u_0^2 k_h^2}, \tag{11}$$

where u_0 is the (constant) background horizontal wind speed and N is the Brunt-Väisälä frequency, which is a measure of atmospheric stability. (Note that for a propagating wave, $N^2 > u_0^2 k_h^2$.)

3.4. Estimates of GLEES Wintertime Soil CO_2 Source Term and Snowpack Fluxes

[38] The observed variations in the undersnow CO_2 do appear to be consistent with pressure-induced advective flows in a dispersive snowpack. However, in order to maintain the observed high levels of mean undersnow CO_2, the soil must be respiring, thereby providing a continuous source of CO_2. The steady state portion of the CO_2 model developed in part 1 of this study indicates that in order to maintain a (more or less) time-invariant CO_2 gradient through the snowpack, the source term, S_χ (ppm s^{-1}), would have to be proportionally greater whenever the snowpack diffusivity, D_e, is augmented by the advectively driven coefficient of dispersion, $\mathcal{D}$. Of course, enhancing D_e by $\mathcal{D}$ would yield proportionally higher CO_2 effluxes from the snowpack as well.

[39] Applying equation (9) and the steady state model of the mean CO_2 data, Table 5 lists the strength of the source term and the flux for the meadow and forest sites for the three model dispersivity types. For the nondispersive case the flux is just the diffusional flux (because the advective flux component, $F_{wave}(0)$, is negligibly small for such low-frequency forcing; see equation (7) or (*Massman* [2006]), but for the dispersive cases the flux is the total flux, which combines the diffusional and dispersive fluxes. To convert S_χ from ppm s^{-1} to μmol-CO_2 m^{-3} s^{-1} we multiplied S_χ (as determined from the model [*Massman*, 2006]) by the molar density of air (c), which can be found from the ideal gas law with the mean ambient pressure (see section 2.1) and the mean soil temperature ($\approx$0.5 C, as reported by *Musselman et al.* [2005]). During the experimental period, c = 30.2 mol-air m^{-3}. The same procedure was followed when converting the fluxes to μmol-CO_2 m^{-2} s^{-1}, except that c is slightly different because the ambient temperature near the snow surface is about -5°C (which is typical for GLEES in the winter).

[40] The results displayed by Table 5 are as expected. However, and more importantly, Table 5 also gives quantitative estimates of the wintertime soil CO_2 source strength (respiration rates) at both a subalpine meadow and forest site. Such results are valuable in and of their own right. In general these results would indicate that the meadow site is biologically more active than forest site, in agreement with *Musselman et al.* [2005].

4. Summary and Conclusions

[41] This paper uses the model of natural atmospheric pressure-induced advective flows within snowpacks and soils developed in part 1 [*Massman*, 2006] to investigate low-frequency fluctuations in CO_2 observed under a deep snowpack in the Rocky Mountains of southern Wyoming. The undersnow CO_2 data were obtained at nearby subalpine forest and meadow sites. Nonharmonic spectral and cospectral analysis techniques were used to show that the spectral characteristics of the wind speed matched those of the undersnow CO_2 better than the ambient pressure. Next, using the wind speed as the forcing variable, the time lag between the forcing at the snow surface and the undersnow CO_2 response was determined and compared with the model's predictions. The results of this study indicate the following.

[42] 1. Advective flows within the snowpack caused by atmospheric pressure fluctuations at the snow surface are responsible for the observed periodic variations in the undersnow CO_2 at the meadow and forest sites.

[43] 2. The wind interacting with the local aerodynamic roughness elements (nearby mountain peaks, forest edges, snowdrifts) creates the surface pressure fields that drive the advective flows.

[44] 3. Thus the low-frequency variations in the wind field modulate the temporal dynamics of the undersnow CO_2, whereas the topography of the site determines the horizontal structure of the wind (pressure) forcing.

[45] 4. Both the forcing by the wind and the response of the undersnow CO_2 are predominantly linear in nature, but both may also contain some weak nonlinear aspects.

[46] 5. The snowpack is no more than weakly dispersive.

[47] 6. Within the subalpine, wintertime CO_2 fluxes emanating from a snowpack and the strength of the soil CO_2 source (respiration rates) may vary significantly between a meadow soil and a forest soil. For this study the meadow soil appears to be more active biologically in the wintertime than the forest soil.

[48] **Acknowledgments.** We would like to thank Mary Albert, Michael Novak, and Thomas Neumann for their many helpful suggestions to this study and this manuscript. Our thanks also go to Bob Hamre, Dick Sommerfeld, and Gene Takle for their scientific and editorial contributions to this manuscript.

References

Albert, M. R., E. F. Schultz, and F. E. Perron Jr. (2000), Snow and firn permeability at Stiple Dome, Antarctica, *Ann. Glaciol.*, *31*, 353–356.

Auer, L. H., N. D. Rosenberg, K. H. Birdsell, and E. M. Whitney (1996), The effects of barometric pumping on contaminant transport, *J. Contam. Hydrol.*, *24*, 145–166.

Chen, C., D. M. Thomas, and R. E. Green (1995), Modeling of radon transport in unsaturated soil, *J. Geophys. Res.*, *100*, 15,517–15,525.

Du Plessis, J. P., and J. H. Masliyah (1991), Flow through isotropic granular porous media, *Trans. Porous Media*, *6*, 207–221.

Holford, D. J., S. D. Schery, J. L. Wilson, and F. M. Phillips (1993), Modeling radon transport in dry, cracked soil, *J. Geophys. Res.*, *98*, 567–580.

Lewicki, J. L., W. C. Evans, G. E. Hilley, M. L. Sorey, J. D. Rogie, and S. L. Brantley (2003), Shallow soil CO_2 flow along the San Andreas and Calaveras Faults, California, *J. Geophys. Res.*, *108*(B4), 2187, doi:10.1029/2002JB002141.

Lundy, C. C., M. Q. Edens, and R. L. Brown (2002), Measurement of snow density and microstructure using computed tomography, *J. Glaciol.*, *48*, 312–316.

Massman, W. J. (2006), Advective transport of CO_2 in permeable media induced by atmospheric pressure fluctuations: 1. An analytical model, *J. Geophys. Res.*, *111*, G03004, doi:10.1029/2006JG000163.

Massman, W. J., R. A. Sommerfeld, R. A. Mosier, K. F. Zeller, T. J. Hehn, and S. G. Rochelle (1997), A model investigation of turbulence-driven pressure-pumping effects on the rate of diffusion of CO_2, N_2O, and CH_4, through layered snowpacks, *J. Geophys. Res.*, *102*, 18,851–18,863.

Millington, R. J. (1959), Gas diffusion in porous media, *Science*, *130*, 100–102.

Musselman, R. C., W. J. Massman, J. M. Frank, and J. L. Korfmacher (2005), The temporal dynamics of carbon dioxide under snow in a high elevation Rocky Mountain subalpine forest and meadow, *Arct. Antarct. Alp. Res.*, *37*, 527–538.

Nappo, C. J. (2002), *An Introduction to Atmospheric Gravity Waves*, Elsevier, New York.

Neale, G. H., and W. K. Nader (1973), Prediction and transport processes within porous media: Diffusive flow processes within an homogeneous swarm of particles, *Am. Inst. Chem. Eng. J.*, *19*, 112–119.

Padmanabhan, G. (1991), Non-harmonic spectral analysis to investigate periodicity in hydrological and climatological time series, *Theor. Appl. Climatol.*, *43*, 31–42.

Schery, S. D., D. H. Gaeddert, and M. H. Wilkening (1984), Factors, affecting exhalation of radon from a gravelly sandy loam, *J. Geophys. Res.*, *89*, 7299–7309.

Schickedanz, P. T., and E. G. Bowen (1977), The computation of climatological power spectra, *J. Appl. Meteorol.*, *16*, 359–367.

Shimizu, H. (1970), Air permeability of temperate snow: Preliminary links to microstructure, *Contrib. Inst. Low Temp. Stud., Ser. A*, *22*, 1–32.

Sommerfeld, R. A., and J. E. Rocchio (1993), Permeability measurements on new and equitemperature snow, *Water Resour. Res.*, *29*, 2485–2490.

Takagi, K., M. Nomura, D. Ashiya, H. Takahashi, K. Sasa, Y. Fujinuma, H. Shibata, Y. Akibayashi, and T. Koike (2005), Dynamic carbon dioxide exchange through snowpack by wind-driven mass transfer in a conifer-broadleaf mixed forest in northernmost Japan, *Global Biogeochem. Cycles*, *19*, GB2012, doi:10.1029/2004GB002272.

Waddington, E. D., J. Cunningham, and S. L. Harder (1996), The effects of snow ventilation on chemical concentrations, in *Chemical Exchange Between the Atmosphere and Polar Snow*, edited by E. W. Wolff and R. C. Bales, pp. 403–451, Springer, New York.

J. M. Frank and W. J. Massman, Rocky Mountain Research Station, USDA Forest Service, 240 West Prospect, Fort Collins, CO 80526, USA. (wmassman@fs.fed.us)